

# Isoindolinium Groups as Stable Anion Conductors for Anion-Exchange Membrane Fuel Cells and Electrolyzers

Kanika Aggarwal, Nansi Gjineci, Alexander Kaushansky, Saja Bsoul, John C. Douglin, Songlin Li, Ihtasham Salam, Sinai Aharonovich, John R. Varcoe, Dario R. Dekel,\* and Charles E. Diesendruck\*



Cite This: *ACS Mater. Au* 2022, 2, 367–373



Read Online

ACCESS |

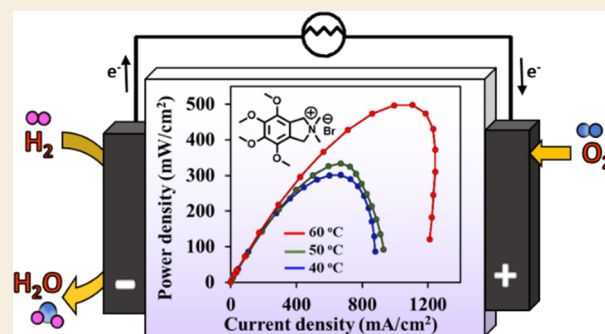
Metrics & More

Article Recommendations

Supporting Information

**ABSTRACT:** Anion-exchange membrane (AEM) fuel cells (AEMFCs) and water electrolyzers (AEMWEs) have gained strong attention of the scientific community as an alternative to expensive mainstream fuel cell and electrolysis technologies. However, in the high pH environment of the AEMFCs and AEMWEs, especially at low hydration levels, the molecular structure of most anion-conducting polymers breaks down because of the strong reactivity of the hydroxide anions with the quaternary ammonium (QA) cation functional groups that are commonly used in the AEMs and ionomers. Therefore, new highly stable QAs are needed to withstand the strong alkaline environment of these electrochemical devices. In this study, a series of isoindolinium salts with different substituents is prepared and investigated for their stability under dry alkaline conditions. We show that by modifying isoindolinium salts, steric effects could be added to change the degradation kinetics and impart significant improvement in the alkaline stability, reaching an order of magnitude improvement when all the aromatic positions are substituted. Density functional theory (DFT) calculations are provided in support of the high kinetic stability found in these substituted isoindolinium salts. This is the first time that this class of QAs has been investigated. We believe that these novel isoindolinium groups can be a good alternative in the chemical design of AEMs to overcome material stability challenges in advanced electrochemical systems.

**KEYWORDS:** isoindolinium, anion-exchange membranes, fuel cells, quaternary ammoniums, electrolyzers



Anion-exchange membranes (AEMs) are based on polymers containing cationic groups that impart anion conductivity in electrochemical devices, such as redox flow batteries, AEM water electrolyzers (AEMWEs), and AEM fuel cells (AEMFCs). AEMFCs and AEMWEs are high-efficiency energy conversion devices with potential applications in the automotive industry, the stationary backup power market, and the storage energy market.<sup>1–6</sup> A limiting issue for the development of these devices is the lack, to date, of AEMs that can withstand the high pH operating conditions, especially at the required elevated temperatures (>80 °C), while maintaining high hydroxide conductivity and good mechanical properties.<sup>7,8</sup> Hence, significant efforts have been made to tackle this challenge by the judicious design of the chemical functional group. Various functional groups have been designed and tested in an effort to increase the alkaline stability, and therefore, the lifetime of AEMs. Strategies include the steric protection of degradation-prone sites<sup>9,10</sup> as well as the use of conformationally restricted structures.<sup>11,12</sup> Early studies from Marino and Kreuer on a broad spectrum of quaternary ammonium (QA)-based cations showed that aliphatic ammoniums generally exhibited greater stability compared to aromatic QAs.<sup>11</sup> In the same study it was

shown that N-spiro-cyclic QAs exhibited the largest stability in 6 M NaOH at 160 °C among the studied molecules, with the best QA being 6-azonia-spiro[5.5]undecane (ASU).<sup>11</sup> The distribution of the positive charge in an aromatic system,<sup>13</sup> such as in imidazolium salts,<sup>14–18</sup> has strongly impacted the QAs' chemical stability toward hydroxide, and further improvements in the membrane lifetime could be achieved by manipulating the imidazolium substituents.<sup>14,19,20</sup>

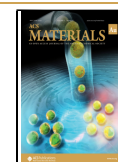
Even though progress has been made in developing QAs that can better withstand alkaline degradation for thousands of hours at high pH and high temperatures, a few studies have been performed under lower hydration or in dry alkaline conditions,<sup>21</sup> which have been shown to better represent conditions occurring during the operation of some electrochemical devices.<sup>22,23</sup> Surprisingly, one of the most studied QAs in the literature, benzyl trimethylammonium (BTMA),

Received: January 3, 2022

Revised: February 6, 2022

Accepted: February 8, 2022

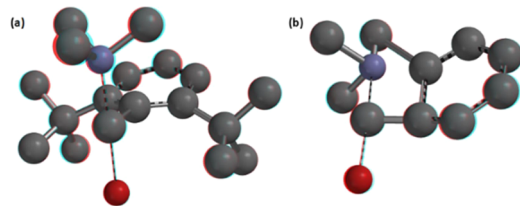
Published: February 23, 2022



which does not perform nearly as well in high temperature and pH, exhibits one of the longest half-lives under dry alkaline conditions at room temperature.<sup>24</sup> In our efforts to address the challenge of designing QA, which is stable toward this harsh dry alkaline condition, a series of carazolium salts with different substituents was prepared,<sup>25,26</sup> and one having N-substituted phenols performed better than BTMA with a half-life of ca. 140 h under completely dry conditions.<sup>27</sup>

Under low hydration conditions, BTMA reacts with hydroxide ions exclusively by nucleophilic attack at the benzylic position.<sup>28</sup> As seen in Scheme 1a, in an ortho-

**Scheme 1. Calculated Transition-State Structures (Density Functional Theory at the B3LYP/631-G\* Level of Theory) for Hydroxide S<sub>N</sub>2 on (a) An Ortho-Substituted BTMA, in Which the Hydroxide Comes from Under the Plane and (b) An Isoindolinium Salt, in Which the Hydroxide Comes at the Same Plane as the Aromatic Ring. Hydrogen Atoms are Omitted for Clarity**



substituted BTMA, the hydroxide can attack perpendicularly to the aromatic ring, and therefore, the substituents cannot create steric effects and further improve the BTMA kinetic stability. However, in the similar isoindolinium salts (Scheme 1b), the additional connection to the aromatic ring locks the nitrogen in place, forcing the hydroxide to approach from the side, in proximity to an ortho substituent. Therefore, in this family of QAs, steric effects can be used to increase the lifetime of the AEM, while maintaining the other good properties of BTMA.

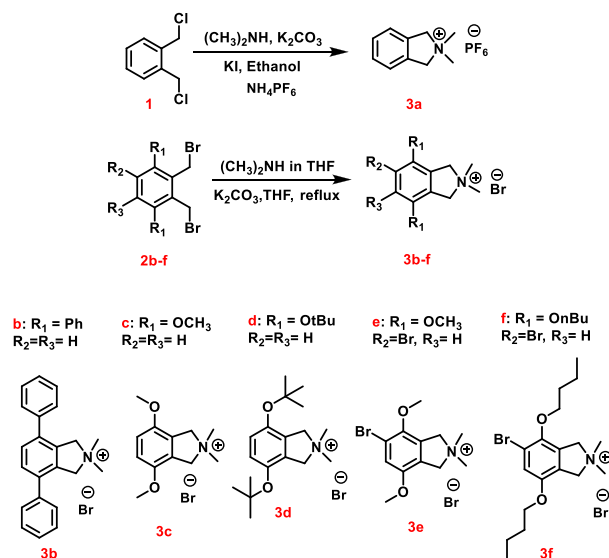
## RESULTS AND DISCUSSION

Chukhadzhyan et al. were the first to synthesize isoindolinium salts by base-catalyzed intramolecular cyclization of ammonium salts containing enyne fragments.<sup>29,30</sup> Dimethyl substituted isoindolinium salts have also been synthesized by a modified Menshutkin reaction.<sup>31,32</sup> For our comparative studies, seven different isoindolinium salts were synthesized (Scheme 2).

The simplest 2,2-dimethylisoindolinium hexafluorophosphate (3a) was prepared by the simple reaction between 1,2-bis(chloromethyl)benzene (1) and dimethylamine. For the substituted isoindolinium salts, different 1,4-substituted-2,3-dimethylbenzenes were brominated using N-bromosuccinimide (NBS) and benzoyl peroxide (BPO) in CCl<sub>4</sub>, providing compounds that are brominated at the benzylic position, and depending on the conditions, also on the phenyl ring (2b–2f).

Cyclization with dimethylamine in tetrahydrofuran (THF) provided the final isoindolinium salts (3b–3f). The alkaline stability of all the isoindolinium salts was tested using the ex-situ protocol previously developed by our group, in which the QAs are measured in dimethyl sulfoxide (DMSO)-d<sub>6</sub> solutions by nuclear magnetic resonance (NMR), and the extent of hydroxide water microsolvation ( $\lambda$ ) is controlled.<sup>28</sup> In these stability tests, the QA concentration was 0.058 M, in a 0.5 M KOH DMSO solution (at a hydration level of ca. 0.1 water

**Scheme 2. Synthetic Procedures Used for the Preparation of Isoindolinium Salts 3a–3f**



molecules per hydroxide). In addition, the alkaline stability of BTMA was also tested for comparison. The results of the kinetics experiments are shown in Figure 1 and Table 1.

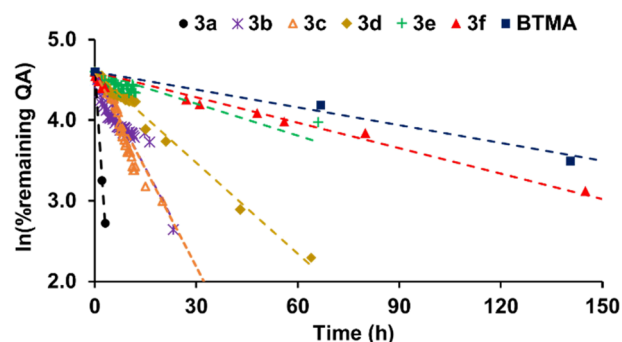


**Figure 1.** Remaining isoindolinium as a function of time during reaction with 0.5 M OH<sup>−</sup> ( $\lambda = 0.1$ ) in DMSO-d<sub>6</sub> at room temperature. The experimental data are fitted with linear trend lines. For comparison, kinetics for the BTMA reaction in the same conditions are also shown.

Because the hydroxide is in large excess (ca. 9 times) compared to the QAs, pseudo-first-order kinetics can be assumed.<sup>24</sup> In this case, the rate constant ( $k$ ) for each QA can be calculated using the equation for first-order reaction kinetics

**Table 1. Pseudo-First-Order Rate Constants and Calculated Half-Lives from the Reaction between Different QAs and Hydroxide**

QA	rate constant (h <sup>−1</sup> )	calculated half-life $t_{1/2}$ (h)
3a	0.63	1.10
3b	0.08	8.77
3c	0.08	8.06
3d	0.04	18.73
3e	$1.30 \times 10^{-2}$	53.32
3f	0.01	69.31
BTMA <sup>24</sup>	$6.38 \times 10^{-3}$	109

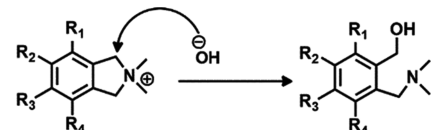
$\ln[QA] = -kt + \ln[QA]_0$ , from the slope of the linear trend lines shown in Figure 1. In the equation,  $[QA]$  refers to the remaining QA fraction at time  $t$ , while  $[QA]_0$  refers to the starting QA fraction (100%). The half-lives were calculated by the equation  $t_{1/2} = \ln(2) \times k^{-1}$ . The rate constants and the calculated half-lives are summarized in Table 1.

As seen in Figure 1, the simple isoindolinium **3a** decomposes very rapidly, with a half-life of only 1 h. This is a significant degradation rate as compared to that measured for BTMA, probably as a consequence of doubling the number of benzylic positions and locking their rotation, allowing for faster attack by hydroxide. The introduction of ortho substituents  $-\text{Ph}$  (**3b**) and  $-\text{OMe}$  (**3c**) lead to ca. 8-fold increase in half-life, to around 8 h. Interestingly,  $-\text{Ph}$  is considered an electron-withdrawing group, while  $-\text{OMe}$  is considered a strong electron-donating group. While both these groups have opposite electronic effects, they both made isoindolinium more stable, suggesting that the source of the effect is steric and not electronic.

On the other hand,  $-\text{OMe}$  groups have been previously shown to stabilize phosphonium salts against attacks by hydroxide through electronic effects.<sup>33</sup> In order to verify this, natural population analysis (NPA) charges (with summed hydrogens) of the benzylic carbons were calculated and found to be 0.224 for **3a** and **3c** (see the Supporting Information (SI)), supporting the fact that the electronic effects of methoxy substituents are negligible in this case, and the origin of stabilization indeed comes from steric rather than electronic effects. The insertion of bulkier groups like *t*-butoxy groups as substituents (**3d**) further improved the stability of the isoindolinium salts, with a further increase in the half-life to 18 h. Still, all these QAs demonstrated inferior stability compared to BTMA. Given that *t*-butoxy groups are already quite bulky, to further improve the steric effect of the substituents in the isoindolinium salts, an additional substituent was added to the fifth position. O-methoxy groups are typically considered to create weak to no steric effects. For example, the pKa of benzoic acid is virtually unaffected by an ortho-methoxy substituent in water or water/DMSO mixtures.<sup>34</sup> The reason behind this is the preference for coplanar conformations of methoxy groups to the aromatic rings, stabilized by mesomeric effects.<sup>35</sup> In our case, the methoxy is coplanar to the aromatic ring and is rotated away from the five-membered ring (also seen in the optimized geometry of **3c**, see DFT calculations below), therefore causing only a minimal steric effect. Interestingly, the presence of an additional substituent in the meta position was shown to lead to conformations in which the methoxy is not coplanar to the aromatic ring, creating stronger ortho steric effects.<sup>35–37</sup> Coincidentally, the 5-bromo substituted **3e** was obtained as a byproduct in the synthesis of **2c**. Upon reaction with dimethyl amine, it provided **3e**, which showed an improved half-life of 53 h. Changing the methoxy to a butoxy substituent (**3f**) further improved the half-life (69 h). Contrary to BTMA,<sup>38,39</sup> in isoindolinium salts, significant effects on stability can be seen by having bulky substituents if their conformations are tuned toward shielding the benzylic carbons.

To better understand and provide guiding concepts on how to further improve the alkaline stability of isoindolinium skeletons, we carried out DFT calculations to evaluate the activation barriers of the hydroxide ion attack to each of the differently substituted substrates (Table 2). Given the multiple conformations possible for each isoindolinium salt and each

**Table 2. Chemical Reaction Studied In Silico; Activation Energies ( $E$  – Electronic,  $H$  – Enthalpy,  $G$  – Gibbs Free Energy) Relative to Corresponding Reactants (kcal/mol)**



QA	<b>3a</b>	<b>3c</b>	<b>3e<sup>a</sup></b>	<b>3e<sup>b</sup></b>	<b>3g</b>
$R_1$	$-\text{H}$	$-\text{OCH}_3$	$-\text{OCH}_3$	$-\text{OCH}_3$	$-\text{OCH}_3$
$R_2$	$-\text{H}$	$-\text{H}$	$-\text{Br}, -\text{H}$	$-\text{Br}, -\text{H}$	$-\text{OCH}_3$
$\Delta E^\ddagger$	14.6	14.6	19.2	14.6	15.7
$\Delta H^\ddagger$	14.0	14.3	18.9	14.3	15.0
$\Delta G^\ddagger$	22.9	23.3	29.5	23.7	24.2

<sup>a</sup>Corresponds to attack on benzylic carbon proximal to bromide.

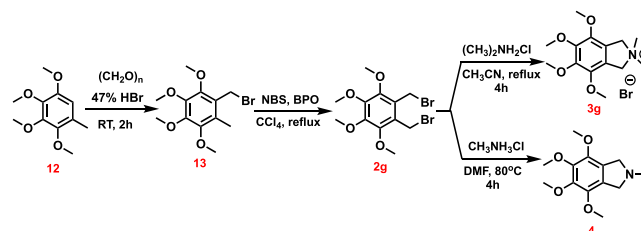
<sup>b</sup>Corresponds to attack on benzylic carbon distal to bromide.

transition state, the structures were initially generated using the CREST computer code developed by Grimme et al. based on semiempirical GFNn-xTB methods (geometries, frequencies, and noncovalent interactions – extended tight-binding).<sup>40</sup> Then, each isomer underwent geometry optimizations (BP86-D3bj/def2-SVP/DMSO) and single point energy calculations (wB97X-D3/def2-TZVP/DMSO). The lowest conformations were chosen, and the relative energies are summarized in Table 2.

The DFT-calculated trends of activation energies are in agreement with our experimental observations. The non-substituted **3a** shows the smallest free energy barrier of 22.9 kcal/mol. Upon addition of the *o*-methoxy groups (**3c**), there is a slight increase to 23.3 kcal/mol. Finally, by adding the bromo substituent at the meta position, a nonsymmetric **3e** is obtained in which attack at the proximal benzylic carbon required 29.5 kcal/mol (**3e<sup>p</sup>**), a quite significant increase. However, the bromo substituent effects on the energy barrier for the attack on the distal benzylic carbon are smaller, reaching 23.7 kcal/mol (**3e<sup>d</sup>**).

These trends are very similar to the experimental observations and suggest that a fully substituted aromatic ring will make isoindolinium salts with significantly higher stabilities toward hydroxide ion attack. To verify this finding, tetramethoxy-substituted isoindolinium (**3g**) was synthesized, as described in Scheme 3. 1,2,3,4-tetramethoxy-5-methylben-

**Scheme 3. Synthetic Procedure Used for the Preparation of Isoindolinium Salts **3g** and **4****



zene (**12**) was reacted with paraformaldehyde in the presence of HBr to provide the bromo monosubstituted precursor **13**. Isoindolinium **3g** was tested under the same dry hydroxide conditions, and the results are shown in Figure 2. The increase in half-life of **3g** is remarkable, achieving 385 h, which is three times higher than that of BTMA<sup>24</sup> and OH carbazolium,<sup>27</sup> the most stable QAs tested under these conditions, and more than

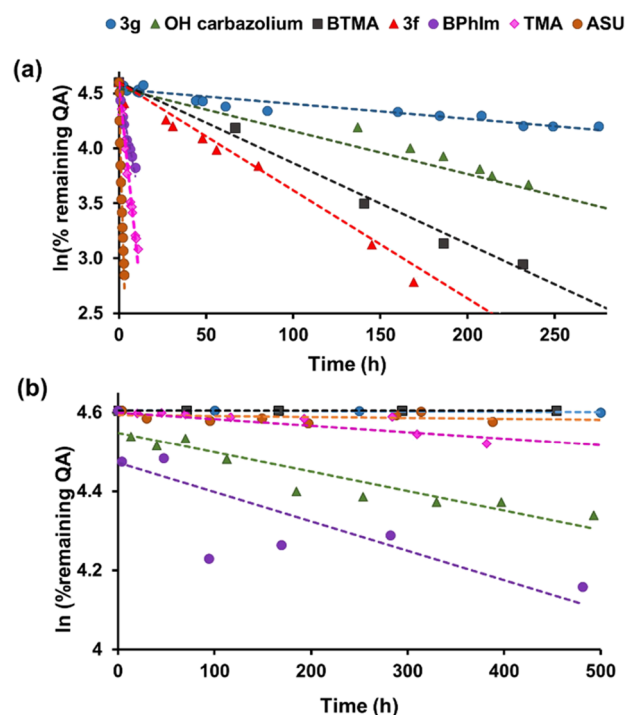


**Figure 2.** Remaining isoindolinium as a function of time during reaction with 0.5 M OH<sup>−</sup> (a)  $\lambda = 0.1$  in DMSO-d<sub>6</sub> at room temperature. (b)  $\lambda = 8$  in DMSO-d<sub>6</sub> at room temperature. The experimental data are fitted with linear trend lines. For comparison, kinetics for BTMA,<sup>24</sup> OH carbazolium,<sup>27</sup> ASU,<sup>11</sup> BPhIm<sup>10,14,44</sup> and TMA reactions under the same conditions are also shown.

five times longer than 3f (Table 3). DFT-calculated activation energies support this increased stability (Table 2). In addition,

**Table 3. Pseudo-First-Order Rate Constants and Calculated Half-Lives from the Reaction between Different QAs and Hydroxide**

QA	water molecule per hydroxide ( $\lambda$ )	rate constant (h <sup>−1</sup> )	calculated half-life $t_{1/2}$ (h)
3f	0	0.01	69
3g	0	$1.80 \times 10^{-3}$	385
	8	$\sim 0$	>34,000
BTMA <sup>24</sup>	0	$6.03 \times 10^{-3}$	109
	8	$\sim 0$	>34,000
OH carbazolium <sup>27</sup>	0	$5 \times 10^{-3}$	139
	8	$4 \times 10^{-4}$	1733
ASU <sup>24</sup>	0	$7.65 \times 10^{-1}$	0.9
	8	$3 \times 10^{-5}$	23,000
BPhIm <sup>24</sup>	0	$7.58 \times 10^{-2}$	9.1
	8	$9 \times 10^{-4}$	770
TMA	0	$7.3 \times 10^{-2}$	9.4
	8	$9.9 \times 10^{-5}$	6931

3g was compared to additional QA salts such as 1,3-di-*n*-butyl-2-(2,6-dimethylphenyl)-4,5-diphenylimidazolium (BPhIm),<sup>24</sup> 6-azonia-spiro[5.5]undecanium (ASU),<sup>24</sup> and tetramethylammonium bromide (TMA),<sup>41</sup> which have been shown to be quite stable under aqueous alkaline conditions (Figure 2 and Table 3).

However, when hydroxide is fully hydrated in its first solvation sphere (Figure 2b,  $\lambda = 8$ ), 3g showed outstanding

stability with no degradation up to 500 h. This result supports the importance of creating efficient steric bulk around both benzylic carbons, as indicated by the DFT calculations, providing a significantly more stable QA.

Then, compound 13 was reacted with NBS and BPO in CCl<sub>4</sub>, to provide the bromo di-substituted compound 2g, which was finally cyclized with dimethylamine to form the desired 3g. Given the outstanding stability of 3g, an AEM containing 3g was prepared for testing in an AEMFC. High-density polyethylene (HDPE) membranes (10  $\mu$ m thick) that were radiation-grafted with 3/4-vinylbenzyl chloride<sup>42,43</sup> were added to a toluene solution of 4 to obtain a tetramethoxy-substituted isoindolinium HDPE (TMISO-HDPE) AEM. The solution was heated to 65 °C for 3 days.

Samples of the obtained TMISO-HDPE AEMs were analyzed by AgNO<sub>3</sub> precipitation titration to measure their ion-exchange capacity (1.28 meq/g). Then, their water uptake (WU) was measured at 40 °C. The membrane showed 27.7% mass increase at 90% relative humidity (RH) and 51.6% of WU at 95% RH. In addition, their ion conductivity was studied after the exchange of the chlorides by hydroxide counter anions by soaking them in a 1 M KOH solution for 1 h (Figure 3).

During the conductivity test, remaining carbonates are converted to hydroxide using the Ziv and Dekel procedure reported elsewhere,<sup>45</sup> upon which a stable ion-conductivity value of 60 mS cm<sup>−1</sup> was obtained at 70 °C. For a stability

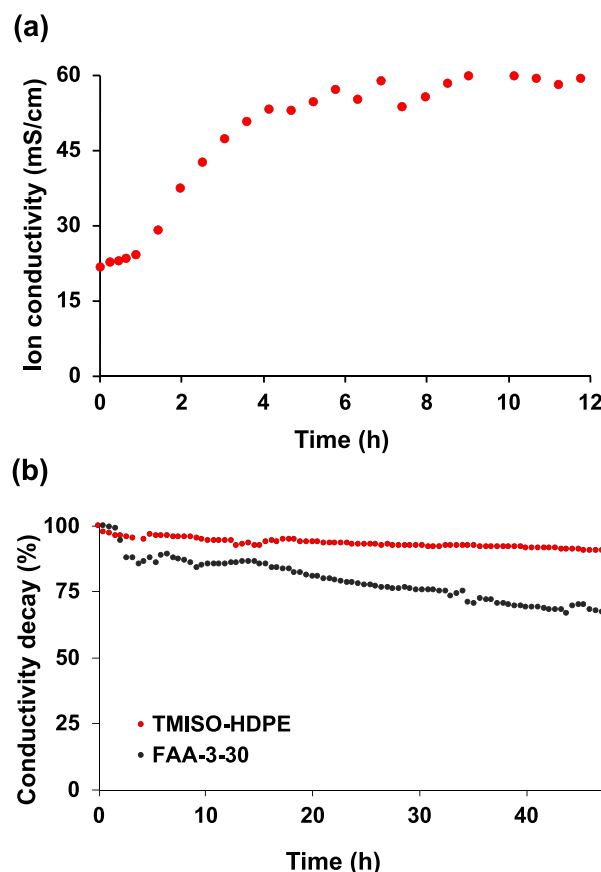


**Figure 3.** (a) Ion conductivity of the TMISO-HDPE AEM measured at 70 °C and 90% relative humidity. (b) Conductivity decay (%) comparison of TMISO-HDPE AEM and commercial FAA-3-30 AEM at 80 °C, 80% RH, under 0.1 mA current and 500 cm<sup>3</sup>/min N<sub>2</sub> flow.

comparison, the conductivity decay of **TMISO-HDPE** and a commercial AEM (FAA-3-30) was measured over time at 80 °C and 80% RH. Both the membranes were immersed in 1 M KOH before the test for 1 h. **TMISO-HDPE** showed only 9% decay, whereas FAA-3-30 presents a more significant 32% decrease in the conductivity after 48 h under the test conditions (Figure 3b).

Finally, larger **TMISO-HDPE** AEM samples were prepared by the same procedure and tested in one of the potential electrochemical devices that require AEM, an AEMFC. Gas diffusion electrodes (5 cm<sup>2</sup>) were prepared according to the method reported elsewhere.<sup>46,47</sup> A H<sub>2</sub>-O<sub>2</sub> AEMFC was tested at cell temperatures of 40, 50 °C without added back-pressurization and of 60 °C with 100 kPa back-pressurization on both the anode and the cathode (Figure 4a). As hydroxide conductivity increases with the temperature, the AEMFC performance increases as well, reaching the best performance at 60 °C, with a peak power density of 497 mW/cm<sup>2</sup>,

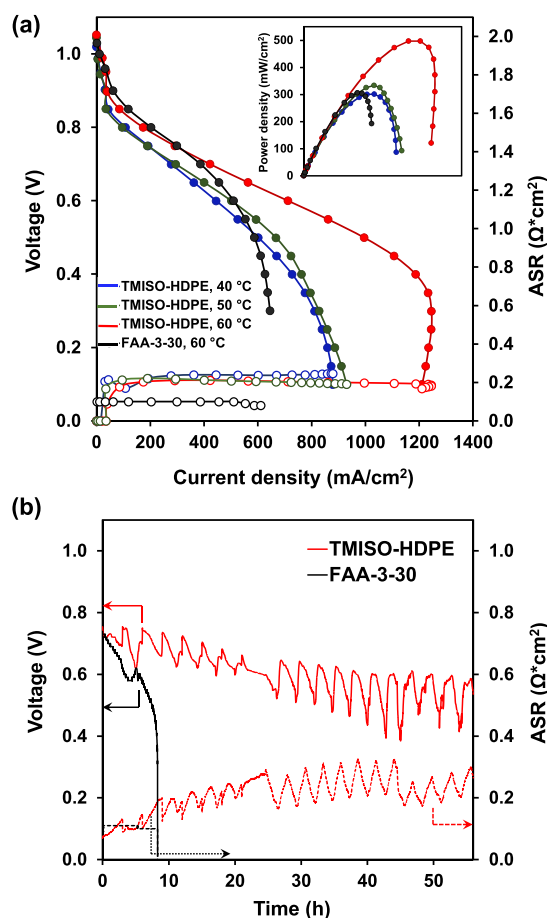


**Figure 4.** (a) Comparison of voltage, area-specific resistance, and power density (insert) vs current density curves of AEMFCs based on the **TMISO-HDPE** AEM and commercial FAA-3-30 AEM. The **TMISO-HDPE** AEM was measured at cell temperatures of 40 and 50 °C with optimized dewpoints and 0 kPa back-pressurization as well as at 60 °C with optimized dewpoints and 100 kPa back-pressurization on both the anode and the cathode. To compare the performance, the commercial FAA-3-30 AEM was also measured at 60 °C under the same cell conditions as the **TMISO-HDPE** AEM. (b) Comparison of the **TMISO-HDPE** AEM and the commercial FAA-3-30 AEM long-term stability test at 60 °C under a constant current density of 300  $\text{mA}/\text{cm}^2$ .

measured at 0.5 V, and a limiting current density of 1210  $\text{mA}/\text{cm}^2$ . At 60 °C, the thin cathode catalyst layer reduced the ability of the cell to retain and distribute back-diffused water, causing the cell to abruptly enter the mass transport region evidenced by the sharp voltage drop of 1000  $\text{mA}/\text{cm}^2$ .<sup>48</sup>

For comparison, an AEMFC made with commercial FAA-3-30 AEM and tested at 60 °C under the same conditions delivered a lower peak power density of 306  $\text{mW}/\text{cm}^2$  and only arrived at a limiting current density of 645  $\text{mA}/\text{cm}^2$ . The average area-specific resistance (ASR) through the **TMISO-HDPE** AEMFC decreased slightly from 0.20 measured at 40 °C to 0.16  $\Omega \cdot \text{cm}^2$  at 60 °C, indicating improved OH<sup>-</sup> conductivity. By comparison, the FAA-3-30 AEMFC showed a slightly improved average ASR of 0.1  $\Omega \cdot \text{cm}^2$  at 60 °C, partly due to the reportedly higher true OH<sup>-</sup> conductivity at that temperature.<sup>49,50</sup> The AEMFCs were additionally subjected to long-term durability testing at 60 °C, under a constant current density of 300  $\text{mA}/\text{cm}^2$ . The **TMISO-HDPE** AEMFC resulted in a voltage degradation rate of 4 mV/h after 56 h, while the voltage of the FAA-3-30 AEMFC dropped to 0 after only 8 h (Figure 4b). The oscillations of the voltage and ASR (Figure 4b) over the measured time in the **TMISO-HDPE** AEMFC are suspected to be due to the nonideal temperature control of gases with the available equipment.

## CONCLUSIONS

Isoindolinium quaternary ammoniums were tested for their alkaline stability under dry conditions. In isoindolinium, the nitrogen substitution is similar to BTMA, but amine rotation is locked, providing the opportunity to create steric effects, leading to increased stability against nucleophilic attack. Seven differently substituted isoindolinium molecules were synthesized, and their stability was tested under harsh dry alkaline conditions. Unsubstituted isoindolinium proved to be less stable than BTMA, probably due to the presence of two benzylic carbons and its cyclic structure locking the methylene rotation. However, as substituents are added, steric effects start to alter the reaction kinetics. When both ortho and meta positions are substituted in the aromatic ring, the half-life is improved drastically. The substitution of the four phenyl positions with methoxy groups provided isoindolinium QA (3g) with a half-life of 385 h under harsh testing conditions, more than three times longer than that of the state-of-the-art BTMA and OH carbazolium. Radiation-grafted HDPE AEMs containing cationic groups based on 3g were prepared and tested, showing good hydroxide ion conductivity and achieving a promising performance in an AEMFC device (even before any significant optimization), showing the great potential of modified isoindolinium groups in electrochemical applications. By studying decomposition reaction pathways and through targeted molecular design, better and improved QA-containing AEMs can be developed. Finally, the lifetime of 3g is the longest reported in the literature up to date under dry alkaline conditions.

## ASSOCIATED CONTENT

### Supporting Information

The Supporting Information is available free of charge at <https://pubs.acs.org/doi/10.1021/acsmaterialsau.2c00002>.

CCDC 2101013 and CCDC 2101014 contain the supplementary crystallographic data for this study. These data can be obtained free of charge from The

Cambridge Crystallographic Data Centre via [www.ccdc.cam.ac.uk/data\\_request/cif](http://www.ccdc.cam.ac.uk/data_request/cif) (PDF)

## AUTHOR INFORMATION

### Corresponding Authors

**Dario R. Dekel** – *The Wolfson Department of Chemical Engineering, Technion – Israel Institute of Technology, 3200003 Haifa, Israel; The Nancy & Stephen Grand Technion Energy Program (GTEP) – Israel Institute of Technology, 3200003 Haifa, Israel;* [orcid.org/0000-0002-8610-0808](https://orcid.org/0000-0002-8610-0808); Email: [dario@technion.ac.il](mailto:dario@technion.ac.il)

**Charles E. Diesendruck** – *Schulich Faculty of Chemistry, Technion – Israel Institute of Technology, 3200008 Haifa, Israel; The Nancy & Stephen Grand Technion Energy Program (GTEP) – Israel Institute of Technology, 3200003 Haifa, Israel;* [orcid.org/0000-0001-5576-1366](https://orcid.org/0000-0001-5576-1366); Email: [charles@technion.ac.il](mailto:charles@technion.ac.il)

### Authors

**Kanika Aggarwal** – *Schulich Faculty of Chemistry, Technion – Israel Institute of Technology, 3200008 Haifa, Israel*

**Nansi Gjineci** – *Schulich Faculty of Chemistry, Technion – Israel Institute of Technology, 3200008 Haifa, Israel*

**Alexander Kaushansky** – *Schulich Faculty of Chemistry, Technion – Israel Institute of Technology, 3200008 Haifa, Israel*

**Saja Bsoul** – *The Wolfson Department of Chemical Engineering, Technion – Israel Institute of Technology, 3200003 Haifa, Israel*

**John C. Douglin** – *The Wolfson Department of Chemical Engineering, Technion – Israel Institute of Technology, 3200003 Haifa, Israel*

**Songlin Li** – *The Wolfson Department of Chemical Engineering, Technion – Israel Institute of Technology, 3200003 Haifa, Israel*

**Ihtasham Salam** – *Department of Chemistry, University of Surrey, Guildford GU2 7XH, U.K.*

**Sinai Aharonovich** – *Schulich Faculty of Chemistry, Technion – Israel Institute of Technology, 3200008 Haifa, Israel*

**John R. Varcoe** – *Department of Chemistry, University of Surrey, Guildford GU2 7XH, U.K.*

Complete contact information is available at: <https://pubs.acs.org/10.1021/acsmaterialsau.2c00002>

### Author Contributions

The manuscript was written through contributions of all authors. K.A. and N.G. contributed equally.

### Notes

The authors declare no competing financial interest.

## ACKNOWLEDGMENTS

This research was sponsored by the RDECOM-Atlantic, US Army Research Office, and the Office of Naval Research Global and was accomplished under Grant Number W911NF-18-1-0322. The views and conclusions contained in this document are those of the authors and should not be interpreted as representing the official policies, either expressed or implied, of the U.S. Government. The U.S. Government is authorized to reproduce and distribute reprints for Government purposes, notwithstanding any copyright notation herein. The radiation-grafted HDPE membranes (preaminated) were

fabricated using funds provided by EPSRC UK (Grant EP/T009233/1). This research was partially supported by the Israel Science Foundation (Grant No. 1934/17).

## REFERENCES

- (1) Varcoe, J. R.; Atanassov, P.; Dekel, D. R.; Herring, A. M.; Hickner, M. A.; Kohl, P. A.; Kucernak, A. R.; Mustain, W. E.; Nijmeijer, K.; Scott, K.; Xu, T.; Zhuang, L. Anion-Exchange Membranes in Electrochemical Energy Systems. *Energy Environ. Sci.* **2014**, *7*, 3135–3191.
- (2) Gottesfeld, S.; Dekel, D. R.; Page, M.; Bae, C.; Yan, Y.; Zelenay, P.; Kim, Y. S. Anion Exchange Membrane Fuel Cells: Current Status and Remaining Challenges. *J. Power Sources* **2018**, *375*, 170–184.
- (3) Stamenkovic, V. R.; Strmcnik, D.; Lopes, P. P.; Markovic, N. M. Energy and Fuels from Electrochemical Interfaces. *Nat. Mater.* **2016**, *16*, 57–69.
- (4) Cano, Z. P.; Banham, D.; Ye, S.; Hintennach, A.; Lu, J.; Fowler, M.; Chen, Z. Batteries and Fuel Cells for Emerging Electric Vehicle Markets. *Nat. Energy* **2018**, *3*, 279–289.
- (5) Li, C.; Baek, J. B. The Promise of Hydrogen Production from Alkaline Anion Exchange Membrane Electrolyzers. *Nano Energy* **2021**, *87*, No. 106162.
- (6) Henkensmeier, D.; Najibah, M.; Harms, C.; Žitka, J.; Hnát, J.; Bouzek, K. Overview: State-of-the Art Commercial Membranes for Anion Exchange Membrane Water Electrolysis. *J. Electrochem. Energy Convers. Storage* **2021**, *18*, No. 024001.
- (7) Dekel, D. R. Review of Cell Performance in Anion Exchange Membrane Fuel Cells. *J. Power Sources* **2018**, *375*, 158–169.
- (8) Tao, Z.; Wang, C.; Zhao, X.; Li, J.; Guiver, M. D. Progress in High-Performance Anion Exchange Membranes Based on the Design of Stable Cations for Alkaline Fuel Cells. *Adv. Mater. Technol.* **2021**, *6*, No. 2001220.
- (9) Mohanty, A. D.; Bae, C. Mechanistic Analysis of Ammonium Cation Stability for Alkaline Exchange Membrane Fuel Cells. *J. Mater. Chem. A* **2014**, *2*, 17314–17320.
- (10) Thomas, O. D.; Soo, K. J. W. Y.; Peckham, T. J.; Kulkarni, M. P.; Holdcroft, S. A Stable Hydroxide-Conducting Polymer. *J. Am. Chem. Soc.* **2012**, *134*, 10753–10756.
- (11) Marino, M. G.; Kreuer, K. D. Alkaline Stability of Quaternary Ammonium Cations for Alkaline Fuel Cell Membranes and Ionic Liquids. *ChemSusChem* **2015**, *8*, 513–523.
- (12) Pham, T. H.; Olsson, J. S.; Jannasch, P. N-Spirocyclic Quaternary Ammonium Ionenes for Anion-Exchange Membranes. *J. Am. Chem. Soc.* **2017**, *139*, 2888–2891.
- (13) Tao, Z.; Wang, C.; Zhao, X.; Li, J.; Ren, Q. High Conductivity and Alkaline Stability of Anion Exchange Membranes Containing Multiple Flexible Side-Chain Piperidinium Ions. *Mater. Chem. Front.* **2021**, *5*, 6904–6912.
- (14) Hugar, K. M.; Kostalik, H. A.; Coates, G. W. Imidazolium Cations with Exceptional Alkaline Stability: A Systematic Study of Structure–Stability Relationships. *J. Am. Chem. Soc.* **2015**, *137*, 8730–8737.
- (15) Fan, J.; Willdorf-Cohen, S.; Schibli, E. M.; Paula, Z.; Li, W.; Skalski, T. J. G.; Sergeenko, A. T.; Hohenadel, A.; Frisken, B. J.; Magliocca, E.; Mustain, W. E.; Diesendruck, C. E.; Dekel, D. R.; Holdcroft, S. Poly(Bis-Arylimidazoliums) Possessing High Hydroxide Ion Exchange Capacity and High Alkaline Stability. *Nat. Commun.* **2019**, *10*, 2306.
- (16) Fan, J.; Wright, A. G.; Britton, B.; Weissbach, T.; Skalski, T. J. G.; Ward, J.; Peckham, T. J.; Holdcroft, S. Cationic Polyelectrolytes, Stable in 10 M KOHaq at 100 °C. *ACS Macro Lett.* **2017**, *6*, 1089–1093.
- (17) Lin, B.; Dong, H.; Li, Y.; Si, Z.; Gu, F.; Yan, F. Alkaline Stable C2-Substituted Imidazolium-Based Anion-Exchange Membranes. *Chem. Mater.* **2013**, *25*, 1858–1867.
- (18) Si, Z.; Qiu, L.; Dong, H.; Gu, F.; Li, Y.; Yan, F. Effects of Substituents and Substitution Positions on Alkaline Stability of

- Imidazolium Cations and Their Corresponding Anion-Exchange Membranes. *ACS Appl. Mater. Interfaces* **2014**, *6*, 4346–4355.
- (19) Lee, B.; Yun, D.; Lee, J. S.; Park, C. H.; Kim, T. H. Development of Highly Alkaline Stable OH-Conductors Based on Imidazolium Cations with Various Substituents for Anion Exchange Membrane-Based Alkaline Fuel Cells. *J. Phys. Chem. C* **2019**, *123*, 13508–13518.
- (20) You, W.; Padgett, E.; MacMillan, S. N.; Muller, D. A.; Coates, G. W. Highly Conductive and Chemically Stable Alkaline Anion Exchange Membranes via ROMP of Trans-Cyclooctene Derivatives. *Proc. Natl. Acad. Sci. U. S. A.* **2019**, *116*, 9729–9734.
- (21) Diesendruck, C. E.; Dekel, D. R. Water – A Key Parameter in the Stability of Anion Exchange Membrane Fuel Cells. *Curr. Opin. Electrochem.* **2018**, *9*, 173–178.
- (22) Dekel, D. R.; Rasin, I. G.; Brandon, S. Predicting Performance Stability of Anion Exchange Membrane Fuel Cells. *J. Power Sources* **2019**, *420*, 118–123.
- (23) Dekel, D. R.; Rasin, I. G.; Page, M.; Brandon, S. Steady State and Transient Simulation of Anion Exchange Membrane Fuel Cells. *J. Power Sources* **2018**, *375*, 191–204.
- (24) Dekel, D. R.; Willdorf, S.; Ash, U.; Amar, M.; Pusara, S.; Dhara, S.; Srebnik, S.; Diesendruck, C. E. The Critical Relation between Chemical Stability of Cations and Water in Anion Exchange Membrane Fuel Cells Environment. *J. Power Sources* **2018**, *375*, 351–360.
- (25) Aharonovich, S.; Gjineci, N.; Dekel, D. R.; Diesendruck, C. E. C. E. An Effective Synthesis of N,N-Diphenyl Carbazolium Salts. *Synlett* **2018**, *29*, 1314–1318.
- (26) Gjineci, N.; Aharonovich, S.; Willdorf-Cohen, S.; Dekel, D. R.; Diesendruck, C. E. The Reaction Mechanism Between Tetraalkylammonium Salts and Hydroxide. *Eur. J. Org. Chem.* **2020**, *2020*, 3161–3168.
- (27) Gjineci, N.; Aharonovich, S.; Dekel, D. R.; Diesendruck, C. E. Increasing the Alkaline Stability of N,N-Diaryl Carbazolium Salts Using Substituent Electronic Effects. *ACS Appl. Mater. Interfaces* **2020**, *12*, 49617–49625.
- (28) Dekel, D. R.; Amar, M.; Willdorf, S.; Kosa, M.; Dhara, S.; Diesendruck, C. E. Effect of Water on the Stability of Quaternary Ammonium Groups for Anion Exchange Membrane Fuel Cell Applications. *Chem. Mater.* **2017**, *29*, 4425–4431.
- (29) Babayan, A. T.; Chukhadzhyan, E. O. Amines and Ammonium Compounds. LXXI. Intramolecular Cyclization of Ammonium Salts with the Formation of Isoindolinium and Benzisoinolinium Salts. *Zhurnal Org. Khimii* **1970**, *6*, 1161–1164.
- (30) Chukhadzhyan, E. O.; Gevorgyan, H. R.; Shahkhatuni, K. G.; Chukhadzhyan, E. O.; Ayrapetyan, L. V.; Khachatryan, A. A. Synthesis of 4-(Hydroxymethyl)Dihydroisoinolinium Salts and Their Intramolecular Recyclization. *Russ. J. Org. Chem.* **2018**, *54*, 517–525.
- (31) Ottenbrite, R. M.; Myers, G. R. A Unique Menschutkin Reaction Involving Fragmentation and Cyclization. *Can. J. Chem.* **1973**, *51*, 3631–3634.
- (32) Arava, S.; Diesendruck, C. E. Strategies for the Synthesis of N-Arylammonium Salts. *Synthesis* **2017**, *49*, 3535–3545.
- (33) Gu, S.; Cai, R.; Luo, T.; Chen, Z.; Sun, M.; Liu, Y.; He, G.; Yan, Y. A Soluble and Highly Conductive Ionomer for High-Performance Hydroxide Exchange Membrane Fuel Cells. *Angew. Chem., Int. Ed.* **2009**, *48*, 6499–6502.
- (34) Hojo, M.; Utaka, M.; Yoshida, Z. Ortho Effects-V. Ortho Effects in the Ionizations of Benzoic Acids in Dimethyl Sulfoxide-Water Mixed Solvents. *Tetrahedron* **1971**, *27*, 2713–2723.
- (35) Vande Velde, C.; Bultinck, E.; Tersago, K.; Van Alsenoy, C.; Blockhuys, F. From Anisole to 1,2,4,5-Tetramethoxybenzene: Theoretical Study of the Factors That Determine the Conformation of Methoxy Groups on a Benzene Ring. *Int. J. Quantum Chem.* **2007**, *107*, 670–679.
- (36) Exner, O.; Fiedler, P.; Budesinsky, M.; Kulhanek, J. Conformation and Steric Effects in Mono- and Dimethoxybenzoic Acids. *J. Org. Chem.* **1999**, *64*, 3513–3518.
- (37) Hattori, T.; Takeda, A.; Suzuki, K.; Koike, N.; Koshiishi, E.; Miyano, S. Accelerating Effect of Meta Substituents in the Ester-Mediated Nucleophilic Aromatic Substitution Reaction. *J. Chem. Soc., Perkin Trans. 1* **1998**, *22*, 3661–3672.
- (38) Long, H.; Pivovar, B. S. Hydroxide Degradation Pathways for Substituted Benzyltrimethyl Ammonium: A DFT Study. *ECs Electrochem. Lett.* **2015**, *4*, F13.
- (39) Nuñez, S. A.; Capparelli, C.; Hickner, M. A. N-Alkyl Interstitial Spacers and Terminal Pendants Influence the Alkaline Stability of Tetraalkylammonium Cations for Anion Exchange Membrane Fuel Cells. *Chem. Mater.* **2016**, *28*, 2589–2598.
- (40) Pracht, P.; Bohle, F.; Grimme, S. Automated Exploration of the Low-Energy Chemical Space with Fast Quantum Chemical Methods. *Phys. Chem. Chem. Phys.* **2020**, *22*, 7169–7192.
- (41) Chempath, S.; Einsla, B. R.; Pratt, L. R.; Macomber, C. S.; Boncella, J. M.; Rau, J. A.; Pivovar, B. S. Mechanism of Tetraalkylammonium Headgroup Degradation in Alkaline Fuel Cell Membranes. *J. Phys. Chem. C* **2008**, *112*, 3179–3182.
- (42) Wang, L.; Peng, X.; Mustain, W. E.; Varcoe, J. R. Radiation-Grafted Anion-Exchange Membranes: The Switch from Low- to High-Density Polyethylene Leads to Remarkably Enhanced Fuel Cell Performance. *Energy Environ. Sci.* **2019**, *12*, 1575–1579.
- (43) Biancolli, A. L. G.; Bsoul-Haj, S.; Douglin, J. C.; Barbosa, A. S.; de Sousa, R. R.; Rodrigues, O.; Lanfredi, A. J. C.; Dekel, D. R.; Santiago, E. I. High-Performance Radiation Grafted Anion-Exchange Membranes for Fuel Cell Applications: Effects of Irradiation Conditions on ETFE-Based Membranes Properties. *J. Membr. Sci.* **2022**, *641*, No. 119879.
- (44) Wang, J.; Gu, S.; Kaspar, R. B.; Zhang, B.; Yan, Y. Stabilizing the Imidazolium Cation in Hydroxide-Exchange Membranes for Fuel Cells. *ChemSusChem* **2013**, *6*, 2079–2082.
- (45) Ziv, N.; Dekel, D. R. A Practical Method for Measuring the True Hydroxide Conductivity of Anion Exchange Membranes. *Electrochem. Commun.* **2018**, *88*, 109–113.
- (46) Douglin, J. C.; Varcoe, J. R.; Dekel, D. R. A High-Temperature Anion-Exchange Membrane Fuel Cell. *J. Power Sources Adv.* **2020**, *5*, No. 100023.
- (47) Kumari, M.; Douglin, J. C.; Dekel, D. R. Crosslinked Quaternary Phosphonium-Functionalized Poly(Ether Ketone) Polymer-Based Anion-Exchange Membranes. *J. Membr. Sci.* **2021**, *626*, No. 119167.
- (48) Gutru, R.; Turtayeva, Z.; Xu, F.; Maranzana, G.; Vigolo, B.; Desforges, A. A Comprehensive Review on Water Management Strategies and Developments in Anion Exchange Membrane Fuel Cells. *Int. J. Hydrogen Energy* **2020**, *45*, 19642–19663.
- (49) Zhegur-Khais, A.; Kubannek, F.; Krewer, U.; Dekel, D. R. Measuring the True Hydroxide Conductivity of Anion Exchange Membranes. *J. Membr. Sci.* **2020**, *612*, No. 118461.
- (50) Mustain, W. E. Understanding How High-Performance Anion Exchange Membrane Fuel Cells Were Achieved: Component, Interfacial, and Cell-Level Factors. *Curr. Opin. Electrochem.* **2018**, *12*, 233–239.